New Light on Disordered Ensembles: *Ab Initio* Structure Determination of One Particle from Scattering Fluctuations of Many Copies

D. K. Saldin,[1,2] H. C. Poon,[1] M. J. Bogan,[3] S. Marchesini,[4] D. A. Shapiro,[5] R. A. Kirian,[6] U. Weierstall,[6] and J. C. H. Spence[6]

[1]*Department of Physics, University of Wisconsin-Milwaukee, Milwaukee, Wisconsin 53211, USA*
[2]*Kavli Institute for Theoretical Physics, University of California, Santa Barbara, California 93106, USA*
[3]*Stanford PULSE Institute, SLAC National Accelerator Laboratory, Menlo Park, California 94025, USA*
[4]*Lawrence Berkeley National Laboratory, Berkeley, California 94720, USA*
[5]*Brookhaven National Laboratory, Upton, New York 11973, USA*
[6]*Department of Physics, Arizona State University, Tempe, Arizona 85287, USA*

(Received 29 September 2010; published 14 March 2011)

We report on the first experimental *ab initio* reconstruction of an image of a single particle from fluctuations in the scattering from an ensemble of copies, randomly oriented about an axis. The method is applicable to identical particles frozen in space or time (as by snapshot diffraction from an x-ray free electron laser). These fluctuations enhance information obtainable from an experiment such as conventional small angle x-ray scattering.

DOI: 10.1103/PhysRevLett.106.115501 PACS numbers: 61.05.cf, 61.05.jm

The overwhelming majority of the known structures at the atomic scale have been determined by x-ray crystallography, a technique which requires crystallization, which may not be possible for all molecules, e.g., many membrane proteins. It is therefore of interest to develop scattering techniques which can determine structures of noncrystallized particles. One such suggestion [1] for the structure determination of single viruses or biomolecules exploits the 10×10^9-fold increase in peak brightness provided by an x-ray free electron laser (XFEL), due to which it may be just possible to detect meaningful signals from single microscopic particles [2,3]. Because of the huge flux of radiation, however, it is possible only to work in the so-called ''diffract-and-destroy'' mode, in which the x-ray pulse must terminate within about 50 fs to avoid resolution-limiting effects resulting from the disintegration of the particle. The difficulty of targeting a single particle in such an experiment could be overcome with the development of a method for extracting structural information from scattering by a disordered ensemble of particles.

The present Letter describes the first experimental demonstration of such a method in a geometry which may be applicable for, e.g., virus particles supported on a flat substrate, or membrane proteins randomly oriented about the surface normal of a black-lipid membrane [4]. Methods of determining the shapes of molecules from solutions in which they are found in random orientations exist already. The method of small angle x-ray scattering (SAXS) does this for biomolecules in solution by modeling the radial dependence of scattered intensities [5]. It has also been suggested [6] that much more information about the molecular structure may be found from minute *angular* fluctuations of the scattered intensities on diffraction patterns from intense radiation of pulse lengths shorter than the rotational diffusion time of the molecules. Similarly, angular intensity fluctuations would also be expected in the scattering of a continuous x-ray beam from stationary particles held, for example, in an ice film. Thus the method described could be generally applicable to particles frozen in either space or time.

The absence of periodicity in the sample means that the scattered x rays form a continuous distribution and is not sampled only at Bragg spots from a crystal, namely, at the Shannon ''frequency'' of the complex amplitudes. The continuous distribution of scattered intensities from the disordered ensemble allows their measurements at their (finer) Shannon angular sampling rate. In turn, such an oversampled distribution [7] allows the structure of the scatterer to be determined by an iterative phasing algorithm [8]. These advantages of signal amplification, damage reduction, and access to oversampled intensities (allowing solution of the phase problem [8]) may be combined if the structure of a single particle may be determined from diffraction patterns from many identical particles with neither translational nor orientational order. The extra information present in the angular correlations allows for an *ab initio* reconstruction free of the modeling and *a priori* assumptions.

We demonstrate here *ab initio* reconstruction of the projection of a single particle in the case of single-axis alignment. Figure 1 is an electron microscope image of about 10 gold nanorods of $\sim$90 nm $\times$ 25 nm lying on their sides in random orientations about the surface normal of a 30 nm thick SiN substrate. The nanorods were purchased from Nanopartz Inc. (nanopartz.com, part number 30-25-750). To prepare individual isolated gold nanorods on the surface, a solution of nanorods was aerosolized via

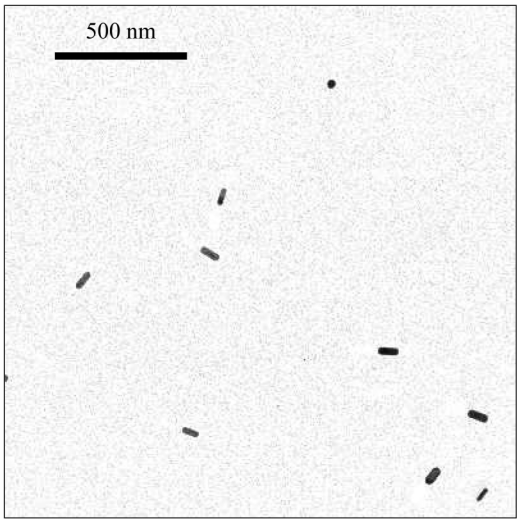

FIG. 1. Transmission electron microscope image of randomly oriented 90×25 nm gold nanorods lying on a SiN substrate, from which soft x-ray diffraction patterns were measured. A particularly dense region is shown for illustration—typical samples consist of approximately 10 gold nanorods per 15 μm^2 region of the SiN substrate. There is a small admixture of ~25 nm diameter gold nanospheres.

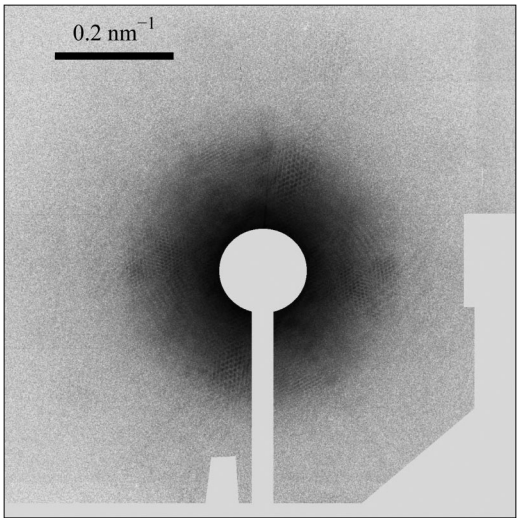

FIG. 2. Measured soft x-ray diffraction pattern from about 10 randomly oriented nanorods on a SiN substrate as in the electron microscope image of Fig. 1.

charge-reduced electrospray and electrostatically captured onto the silicon nitride membrane using previously described methods [9]. The size variation in both length and diameter of the nanorods was approximately 10%–15% in both dimensions, but a small but significant fraction (~ 20%) of the nanoparticles were spherical in shape. We collected soft-x-ray transmission diffraction patterns at beam line 9.0.1 of the Advanced Light Source (ALS) using 750 eV highly coherent x rays (1.65 nm wavelength). Hundreds of diffraction patterns were collected from different 15-micron diameter regions, each containing approximately 10 ± 5 nanorods. During these many hours of automated data recording (with computer-controlled sample stage motions for each new region) the intensity of the x-ray source steadily decreased to approximately one third of the initial intensity. A typical diffraction pattern from a region of the sample containing about 10 nanorods is shown in Fig. 2.

Angular correlation functions $C_2(q, q'; \Delta\phi)$ were formed from each of these multiparticle diffraction patterns, following the prescription [10]:

$$C_2(q, q'; \Delta\phi) = \left\langle \frac{1}{N_\phi} \sum_j I'(q, \phi_j) I'(q', \phi_j + \Delta\phi) \right\rangle_{\mathrm{DP}} \quad (1)$$

where N_ϕ is the number of azimuthal angles ϕ_j at which the intensities are measured, and the angular brackets denote an average over diffraction patterns (DP),

$$I'(q, \phi_j) = I(q, \phi_j) - I_{\mathrm{SAXS}}(q) \quad (2)$$

where $I_{\mathrm{SAXS}}(q)$ is the average intensity over a resolution ring q, and

$$I'(q', \phi_j + \Delta\phi) = I(q', \phi_j + \Delta\phi) - I_{\mathrm{SAXS}}(q'). \quad (3)$$

It has been shown [10] that a sum of many such correlation functions from different sets of randomly oriented particles converges to that from a single particle.

The angular Fourier transform of C_2, may be written [10–12]

$$B_M(q, q') = \frac{1}{N_\phi} \sum_{\Delta\phi} C_2(q, q', \Delta\phi) e^{-iM\Delta\phi} = N_p I_M(q) I_M^*(q') \quad (4)$$

where N_p is the number of scatterers contributing to the measured diffraction pattern, and $I_M(q)$ are (generally complex) the circular harmonic expansion coefficients of a single-particle diffraction pattern

$$I(q, \phi) = \sum_M I_M(q) \exp(iM\phi) \quad (5)$$

where (q, ϕ) are the polar coordinate representation of the 2D scattering vector $\mathbf{q}$, and where the condition $I_{-M}(q) = I_M^*(q)$ ensures the reality of the diffraction intensities $I(q, \phi)$.

The magnitudes of the circular-harmomic expansion coefficients are easily recovered from the angular Fourier transforms (4) since this equation implies that

$$|I_M(q)| = \frac{1}{N_p} \sqrt{B_M(q, q)}. \quad (6)$$

In general [10–12] it is necessary to recover also the phases of these complex coefficients. However, for the diffraction pattern of an object with a long thin rectangular projection, we argue that these phases are most likely to be zero.

To see why this is so, imagine such an object oriented with its long axis along the y direction of a 2D Cartesian

coordinate in the plane parallel to the particle cylinder axes. The Fourier transform of a rectangular projection of the electron density of such an object has the appearance of two mutually perpendicular sets of sinc functions, with the finer fringes parallel to the short axis of the rod projection (the q_x axis) and the broader fringes parallel to the q_y axis. Thus, the brightest fringe on the diffraction pattern will be along the q_x axis, i.e., the axis along which $\phi = 0$ and π radians. Also, since q_x is an axis of symmetry, $I(q, \phi) = I(q, -\phi)$. Consequently,

$$I_M(q) = \int I(q, \phi) \exp(-iM\phi) d\phi = \int I(q, \phi) \cos(M\phi) d\phi \quad (7)$$

and all the $I_M(q)$ coefficients are real. In addition, since for this particular diffraction pattern, the intensities near $\phi = 0$ and π will be dominant, the positive values of the integrand near $\phi = 0$ and π will be dominant. (Friedel's Law implies that the $I_M(q)$ coefficients are nonzero only for even M [10], and thus $\cos(M\pi)$ will be positive.) Thus, the angular integral (7) is overwhelmingly likely to be positive. This means that if the $I_M(q)$'s are treated as complex coefficients, they will be highly likely to have zero phases. This conclusion was confirmed by explicit calculations of the $I_M(q)$ coefficients of a model rod oriented along the y axis using an analytical expression [10] for the diffracted intensities.

Thus, in the case of a rodlike object, its diffraction pattern may be reconstructed from expression (5) once the magnitudes $|I_M(q)|$ are found from (6) since all their phases may be taken as zero. This is quite analogous to the case of conventional crystallography and a centrosymmetric structure with a heavy atom at the center of symmetry [13] which may be considered to give rise to scattered amplitudes with zero phases.

We evaluated [10] the angular correlations $C_2(q, q, \Delta\phi)$ from 121 measured diffraction patterns of the form of Fig. 2, and computed their average according to (1). Prior to extraction of angular correlations, each frame was background subtracted in order to remove intensity due to small low-angle contribution of the SiN substrate and stray light. We then found the magnitudes $|I_M(q)|$ of the circular harmonic expansion coefficients from the angular Fourier transform (4) and from (6). The single-particle diffraction pattern reconstructed from these real coefficients using (5) is shown in Fig. 3. The light circle in the center represents the region of the beam stop.

Because of the possibility of scattering contributions from objects external to the nanorod, we included only circular harmonic expansion coefficients $I_M(q)$ that could have come from scattering by an object generously estimated to have a radius $R \sim 80$ nm, namely, those for which $M < qR$, approximately [14]. Figure 4 shows the same diffraction pattern after 100 iterations of the phasing algorithm. The quality of the reconstruction is judged by smoothness of the interpolation of the intensities in the central beam stop. Figure 5 shows an image of the projected structure of a single nanorod reconstructed simultaneously (this is the real-space image corresponding to the reconstructed single-particle diffraction pattern in Fig. 4. Because of the random-phase starting point, no two reconstructed images are identical. However, essentially the same reconstructed image of the gold rod results when there is smooth interpolation of the missing intensities in the beam stop (apart from the random position within the

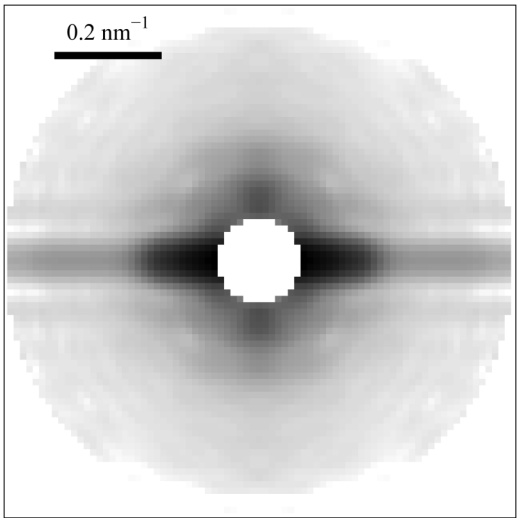

FIG. 3. Single-particle diffraction pattern reconstructed from the angular correlations of 121 measured multiparticle diffraction patterns of the form of Fig. 2. The maximum value of the momentum transfer vector in this pattern was determined by the largest reasonably complete resolution ring of the measured multiparticle diffraction pattern corresponding to $q = 0.471$ nm^{-1}.

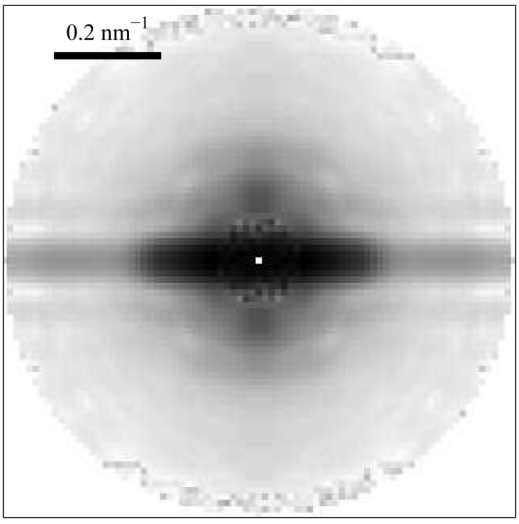

FIG. 4. Reconstructed single-particle diffraction pattern after 100 iterations of the phasing algorithm. This is essentially the same as that of Fig. 3, except that it contains estimations of the missing intensities in the beam stop.

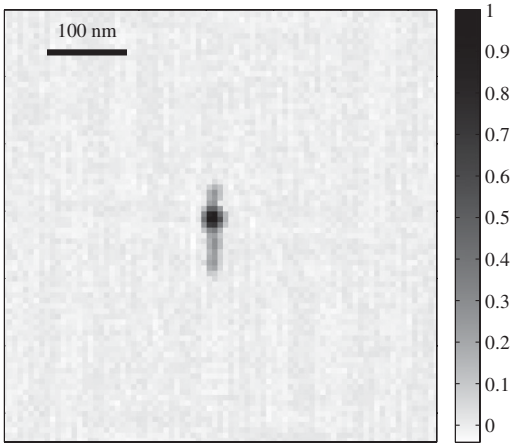

FIG. 5. Projection of the electron density of a single ~90 nm × 25 nm rod reconstructed from the diffraction pattern of Fig. 3 after 100 iterations of the reciprocal-to-real-space phasing algorithm. The nominal resolution corresponding to 2π divided by the maximum magnitude of the scattering vector q in Fig. 3 is about 13 nm. The bulge near the center is probably a superposition of an image of a nanosphere, also found in the experimental samples (see Fig. 1). A scale bar for the reconstructed electron density is shown to the right of the figure.

image frame of the reconstructed projection of the gold rod). The imperfection of the reconstructed image is probably due to the admixture of some gold nanospheres, as apparent from the TEM image of Fig. 1. Since the diffraction from spheres lacks angular fluctuations, the resulting diffraction pattern reconstructed by our algorithm is the number-weighted incoherent superposition of both rod and sphere diffraction patterns.

The final step in the single-particle structure determination is the reconstruction of a single-particle real-space image from this pattern. We did this with a charge-flipping [15] and phase-shifting [16] iterative phasing algorithm. According to the prescription of Oszlànyi and Süto, we began with diffraction amplitudes whose magnitudes $|A(\mathbf{q})|$ are taken to be $\sqrt{I(\mathbf{q})}$, the intensities from Fig. 3, and random phases. The 2D Fourier transform of this yielded an initial estimate of the electron density. The charge-flipping prescription [15] then modifies this electron density by flipping (i.e., changing the signs of) electron density values below ~4% of the maximum. An inverse Fourier transform of this modified electron density then gives a new estimate of the phases associated with the diffraction amplitudes $A(\mathbf{q})$. The magnitudes $|A(\mathbf{q})|$ are replaced by their known values from Fig. 3, but are unaltered in the region of the beam stop where the magnitudes are assumed unknown (this allows the unknown magnitudes to be estimated from constraints in both real and reciprocal space). In addition, the phases of the so-called "weak reflections" (i.e., those below about 4% of the maximum intensity) are shifted by $\pi/2$ radians [16], and the whole process iterated to convergence.

By allowing the diffraction intensities in the region of the beam stop in Fig. 3 to "float" during the course of the iterations, they are estimated at the same time as the image is reconstructed. The continuity of the interpolated intensities with those directly reconstructed from the angular correlations was taken to be an indication of the correctness of any particular reconstruction, as in Fig. 4. A typical real-space image reconstructed after 100 iterations of the phasing algorithm is shown in Fig. 5.

In conclusion, we have demonstrated the first experimental *ab initio* image reconstruction of a single particle from the diffraction pattern of an ensemble of randomly oriented copies from its angular correlations. The results show that effects of interparticle interference from the partially coherent incident radiation are essentially negated if the particles are also in random positions. They also show the robustness of the method to some variations of particle size and shape. These results were also confirmed by simulations with radiation of a 2 μm coherence length expected from radiation from the Advanced Light Source at Berkeley, and a Gaussian distribution of particle sizes with a standard deviation of 10%. The sizes of the nanoparticles in our experiment are approximately that of a typical virus, suggesting a possible application to structure determination of virus particles supported on a similar substrate.

The data were measured at the ALS, supported by DOE Contract No. DE-AC02-05CH11231. D. K. S. was supported by NSF Grant No. PHY05-51164 to the Kavli Institute for Theoretical Physics and M. J. B. through the PULSE Institute for Ultrafast Energy Science at the SLAC National Accelerator Laboratory by the DOE. D. K. S. and JCHS jointly acknowledge support from DOE Grant No. DE-SC0002141.

[1] R. Neutze *et al.*, Nature (London) **406**, 752 (2000).
[2] R. Fung *et al.*, Nature Phys. **5**, 64 (2008).
[3] N. T. D. Loh and V. Elser, Phys. Rev. E **80**, 026705 (2009).
[4] A. Beerlink *et al.*, Langmuir **24**, 4952 (2008).
[5] M. V. Petoukhov and D. I. Svergun, Curr. Opin. Struct. Biol. **17**, 562 (2007).
[6] Z. Kam, Macromolecules **10**, 927 (1977).
[7] J. W. Miao *et al.*, Nature (London) **400**, 342 (1999).
[8] S. Marchesini, Rev. Sci. Instrum. **78**, 049901 (2007).
[9] M. J. Bogan *et al.*, J. Aerosol Sci. **38**, 1119 (2007).
[10] D. K. Saldin *et al.*, New J. Phys. **12**, 035014 (2010).
[11] D. K. Saldin *et al.*, Phys. Rev. B **81**, 174105 (2010).
[12] H. C. Poon and D. K. Saldin, Ultramicroscopy (to be published).
[13] W. L. Bragg, Nature (London) **143**, 678 (1939).
[14] E.g., J. B. Pendry, *Low Energy Electron Diffraction* (Academic Press, London, 1974).
[15] G. Oszlànyi and A. Süto, Acta Crystallogr. Sect. A **60**, 134 (2004).
[16] G. Oszlànyi and A. Süto, Acta Crystallogr. Sect. A **61**, 147 (2005).